Chemical Geology 353 (2013) 280–302

Contents lists available at ScienceDirect

Chemical Geology

journal homepage: www.elsevier.com/locate/chemgeo

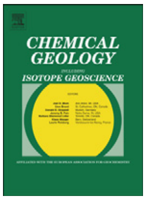

Geochemistry, mineralogy and petrology of the Eocene potassic magmatism from the Milk River area, southern Alberta, and Sweet Grass Hills, northern Montana

Alexei S. Rukhlov [a,*], Alexandra I. Blinova [b], John G. Pawlowicz [a]

[a] Alberta Geological Survey, Energy Resources Conservation Board, Twin Atria Building, 4999-98th Avenue, Edmonton, Alberta, Canada T6B 2X3
[b] Department of Earth and Atmospheric Sciences, University of Alberta, Edmonton, Alberta, Canada T6G 2E3

ARTICLE INFO

Article history:
Accepted 8 October 2012
Available online 15 October 2012

Keywords:
Olivine minette
Lamproite
Fractional crystallization
Wyoming craton
Metasomatized lithospheric mantle
Mesoproterozoic mantle upwelling

ABSTRACT

New whole-rock geochemical, quantitative mineralogical and electron-microprobe data are presented from lamproite, olivine minettes and mafic trachyte of the Milk River area, southern Alberta, and latites, trachytes and high-K rhyolite of the Sweet Grass Hills, northern Montana. These rocks comprise dikes, small plugs and a pipe complex associated with mainly syenite and hornblende monzonite plutons that core several buttes in the Sweet Grass Hills and mark the northern extent of the Cenozoic Montana Alkaline Province. Minerals restricted to peralkaline lamproite at the 49th Parallel locality include Ti-rich phlogopite–annite with Fe^{3+} in tetrahedral coordination, Na-poor sanidine, Ba-rich and Cl-poor fluorapatite, K-rich titano-ferronyböite/ferro-obertiite, LREE-rich strontian fluorapatite ($SrO = 17.5–25.2$ wt.%, $Ce_2O_3 = 2.9–3.3$ wt.%), ilmenite, strontian barite, barian celestine, and unidentified Zr–Ti phase ($TiO_2 = 76.7–88.0$ wt.%, $ZrO_2 = 2.1–7.2$ wt.%) perhaps replacing primary Zr–Ti silicates. The strontian fluorapatite has the highest SrO content thus far reported in the literature for apatites from lamproites. Olivine minettes and mafic trachyte of the Milk River area contain augite, Al-diopside, Ti-rich magnetite, sanidine with higher Na, hyalophane, Cl-bearing fluorapatite with negligible Ba, ferroan magnesite phenocrysts, and primary calcite, all of which are notably absent in the 49th Parallel lamproite. Mica displays distinct core-to-rim zoning trends in these rocks, characterized by increasing FeO_t and TiO_2 at decreasing Al_2O_3 in lamproite and increasing FeO_t and TiO_2 at increasing Al_2O_3 in minettes and trachytes. The 49th Parallel lamproite has higher Ti, K, P, Ba, Rb, Sr, Nb, Th, U, Zr, Hf and REE concentrations, higher K/Al, $(Ce/Yb)_{CN}$, $(La/Sm)_{CN}$, $(Gd/Yb)_{CN}$, Rb/Cs, Ce/Pb, Th/Ta, Th/Yb, and lower Ba/La, Ba/Th and Nb/U relative to minettes of the Milk River area. Major-element, least-squares mass balance and trace-element models call for the origin of latites, trachytes and high-K rhyolite in the Sweet Grass Hills complex by two-stage fractional crystallization of primitive olivine minette magmas concurrent with negligible, if any, assimilation of crustal materials. Oscillatory and reverse zoning in phenocrysts and hybrid phenocryst assemblages record recharge of more evolved magma chambers with primitive minette magmas. The calculated evolutionary models are inconsistent with the compositional variations displayed by the olivine minettes and lamproite of the Milk River area. These rocks represent distinct low-degree partial melts of sub-lithospheric mantle enriched in K and volatiles by the recent (<100 Ma) plume activity or convective upwelling of the upper mantle above subducted Farallon slab, which underwent variable assimilation of the ancient, LREE-Ba–Sr enriched and HFSE depleted Wyoming–Medicine Hat lithosphere during the post-Laramide extension. The olivine minettes derived from more oxidized, carbonated region of the mantle source, compared to the more reduced source of the 49th Parallel lamproite. The extremely negative εNd values, unradiogenic Pb and moderately radiogenic Sr isotopic compositions, correlated with LREE, Ba enrichment and relative Nb, Ta, Ti and other HFSE depletions of the Cenozoic K-rich rocks of the MAP, may reflect carbonatite metasomatism of the lithospheric mantle associated with the widespread Mesoproterozoic (1.5–1.4 Ga) anorogenic magmatism and intracontinental rifting related to mantle upwelling and plume activity beneath a thick Precambrian supercontinent.

1. Introduction

A wide range of petrologic rock types is present within the Late Cretaceous–Oligocene (75–28 Ma) Montana alkaline province (MAP) and environs (e.g., Pirsson, 1905; Larsen, 1940; Currie, 1976; Hearn et al., 1978; Marvin et al., 1980; Irving and Hearn, 2003). The majority are potassic alkaline rocks (e.g., syenites, monzonites, latites,

---

[*] Corresponding author at: British Columbia Geological Survey, PO Box 9333 Stn Prov Gov't, 5th Floor 1810 Blanshard St., Victoria, British Columbia, Canada V8W 9N3. Tel.: +1 250 952 0396; fax: +1 250 952 0381.
E-mail address: Alexei.Rukhlov@gov.bc.ca (A.S. Rukhlov).

0009-2541/$ – see front matter. Crown Copyright © 2012 Published by Elsevier B.V. All rights reserved.
http://dx.doi.org/10.1016/j.chemgeo.2012.10.024

minettes, lamproites, leucite phonolites, ultramafic lamprophyres and kimberlites) with subordinate sodic alkaline rocks (e.g., alkali olivine basalts, basanites, olivine nephelinites) and a few carbonatite occurrences (Irving and Hearn, 2003). Their Sr–Pb–Nd isotopic signatures define arrays on the isotope ratio correlation diagrams, scattering from near bulk Earth composition, or the Focus Zone (FOZO) mantle (Hart et al., 1992; Hauri et al., 1994; Campbell and O'Neill, 2012) towards extremely unradiogenic ^{143}Nd/^{144}Nd, ^{206}Pb/^{204}Pb, and ^{208}Pb/^{204}Pb but only moderately radiogenic ^{87}Sr/^{86}Sr, quite unlike K-rich volcanic rocks of Mediterranean, E. Africa, W. Australia and Antarctica which have more radiogenic Sr, Pb and Nd isotopic compositions (e.g., Vollmer et al., 1984; Fraser et al., 1985; Nelson et al., 1986; Dudás et al., 1987; Irving and O'Brien, 1991; Macdonald et al., 1992; O'Brien et al., 1995). Proposed models for the origin of Cenozoic potassic rocks of the Montana alkaline province involve mixing of at least two components in the source region of their parental magmas: an asthenospheric mantle enriched in volatiles and potassium by the recent (<100 Ma) hotspot activity or convectively upwelling mantle above the Farallon slab, and an ancient lithospheric mantle enriched in light rare earth elements (LREE) and large ion lithophile elements (LILE), with relative depletions in Nb, Ta, Ti and other high field strength elements (HFSE) (e.g., Dudás et al., 1987; Meen and Eggler, 1987; Eggler et al., 1988; Hearn et al., 1991; O'Brien et al., 1991, 1995; Scambos, 1991; Macdonald et al., 1992; Carlson et al., 1999; Buhlmann et al., 2000; Greenough and Kyser, 2003; Carlson et al., 2004; Downes et al., 2004; Mirnejad and Bell, 2006). Although isotopic data from mantle xenoliths constrain the Mesoproterozoic timing for the LREE enrichment of the Wyoming lithosphere (Dudás et al., 1987; Carlson and Irving, 1994; Carlson et al., 1999, 2004), the nature of this metasomatism remains unknown (Downes et al., 2004). Compositional variations within the individual complexes were also attributed to evolutionary processes involving fractional crystallization, magma mixing, phenocryst accumulation and crustal assimilation (e.g., Leat et al., 1988a; O'Brien et al., 1991; Macdonald et al., 1992; Kjarsgaard, 1997; Buhlmann et al., 2000; Feeley and Cosca, 2003; Greenough and Kyser, 2003).

The Eocene potassic igneous complex, composed of mafic to felsic intrusions in the Sweet Grass Hills, Montana and subordinate exposures to the north in the Milk River area, Alberta, stands out because it marks the northern limit of the MAP and shows a range of rock types that can be analyzed to test the petrogenetic models (Truscott, 1975; Lopez, 1995; Kjarsgaard, 1997; Buhlmann et al., 2000; Irving and Hearn, 2003). Kjarsgaard (1997, 1994) described all mica-rich igneous rocks in the Milk River area as minettes. Compositional variations between minettes of the Milk River area were attributed to fractional crystallization and ponding of magma, along with mixing and crystal accumulation (Kjarsgaard, 1997; Buhlmann et al., 2000). However, these models do not explain: 1) the origin of intermediate and felsic rocks in the Sweet Grass Hills igneous complex, 2) contrasting mineralogy and mineral chemistry of the ultrapotassic rocks in the Milk River area, and 3) different LREE enrichment, incompatible-element ratios and Sr–Pb–Nd isotopic signatures between these rocks. Therefore, the objective of this study is to evaluate the origin of ultrapotassic rocks of the Milk River area and magmatic evolution within the Sweet Grass Hills igneous complex using available experimental evidence and quantitative geochemical models based on the new geochemical and mineralogical evidence and published data. We synthesize the new geochemical and published isotopic characteristics from the Milk River ultrapotassic rocks and other Cenozoic complexes of the MAP to discuss the nature of the mantle source of their parental magmas, its time-integrated LREE enrichment and relative Nb, Ta, Ti and other HFSE depletions, and the tectonic context of its evolution.

2. Geology and tectonic setting

Details of geology of the Sweet Grass Hills igneous complex and tectonic setting of the MAP are summarized in Rukhlov and Pawlowicz (2012). The Eocene Sweet Grass Hills igneous complex is emplaced into the Carboniferous, Jurassic and Cretaceous limestones, shales and siliciclastic strata underlain by the Archean Medicine Hat crystalline basement (3.28–2.61 Ga) to the east of the Cordilleran Foreland fold-and-thrust belt (Fig. 1; Marvin et al., 1980; Ross et al., 1991; Villeneuve et al., 1993; Lopez, 1995). It consists of mainly monzonite and syenite plutons and dikes, sills and small plugs made up of potassic lamprophyres, latites, trachytes and felsite breccia (Truscott, 1975; Currie, 1976; Kjarsgaard, 1994; Lopez, 1995, 2002; Irving and Hearn, 2003). Pyroclastic and epiclastic rocks are preserved within a pipe complex at Coulee 29 locality to the north of Sweet Grass Hills in the Milk River area (Fig. 1a; Burwash and Nelson, 1992; Kjarsgaard, 1994; Walker, 1994). The majority of igneous rocks in the Milk River area are olivine minettes, with subordinate mafic trachyte, latite and lamproite (e.g., Kjarsgaard, 1997; Buhlmann et al., 2000; Rukhlov and Pawlowicz, 2012).

On a regional scale, much of the MAP and the coeval Challis calc-alkaline volcanic field (49–44 Ma) to the southwest are underlain by the Mesoproterozoic Belt–Purcell basin and the northeast-trending Proterozoic Great Falls Tectonic Zone (GFTZ) (Fig. 1b). The GFTZ separates the Archean Medicine Hat basement to the north from the Archean Wyoming craton to the south (O'Neill and Lopez, 1985; Ross et al., 1991; Vuke et al., 2007). However, the Sweet Grass Hills igneous complex is isolated to the north of the GFTZ and the main part of the MAP, on the east flank of the Sweetgrass Arch (Fig. 1; Lopez, 1995). A northwesterly alignment of the Sweet Grass Hills intrusions may reflect emplacement controlled by reactivation of the basement structures during the regional Eocene extension (Lopez, 1995).

Numerous tectonic models involving Farallon plate subduction and Yellowstone plume have been proposed for the MAP and environs (e.g., Eggler et al., 1988; Thorkelson and Taylor, 1989; O'Brien et al., 1991, 1995; Baker, 1992; Christiansen et al., 2002; Dostal et al., 2003; Madsen et al., 2006; Mirnejad and Bell, 2006). All of these models require interaction between ancient lithospheric mantle, inferred to have been metasomatized by LREE-Ba–Sr-rich and Nb, Ta, Ti, Hf and Zr depleted melts/fluids in Mesoproterozoic, and asthenospheric mantle providing heat and Rb–K-rich volatile influx due to dehydration of the Farallon slab or mantle plume (e.g., Dudás, 1991; Macdonald et al., 1992; Edgar and Mitchell, 1997;Buhlmann et al., 2000; Downes et al., 2004; Mirnejad and Bell, 2006).

3. Analytical techniques

Details of the analytical methods are given in Appendix A, Electronic Supplement. Quantitative Rietveld X-ray diffraction (XRD) and mineral-liberation analyses (MLA) were performed at Activation Laboratories Ltd. (Appendix B, Electronic Supplement). Chemical compositions of minerals were analyzed in polished thin sections by a JEOL 8900 electron microprobe using five wavelength dispersive spectrometers at University of Alberta (Appendix C, Electronic Supplement). The back-scattered electron (BSE) images and elemental X-ray maps were obtained using a CAMECA SX100 electron microprobe in the same laboratory. Structural formulas were calculated using modified sub-routines in CALCMIN (Brandelik, 2009). Whole rock major- and trace-element analyses were performed at Acme Analytical Laboratories Ltd. Tables 2 and 3 list the representative major- and trace-element whole rock data, respectively. Complete datasets by different methods can be found in Rukhlov and Pawlowicz (2012).

For internal data-quality control, we analyzed six splits (30–72 g) of the Canadian Certified Reference Materials Project (CCRMP) TDB-1 rock standard (http://www.nrcan.gc.ca/minerals-metals/technology/certified-reference-materials/certificate-price-list/3380). The six splits of the TDB-1 were weighed into plastic vials and randomly inserted in sample sets before the samples were sent to the laboratory. The average and relative standard deviation (RSD %) values of the TDB-1 analyses provide accuracy and reproducibility controls (Tables 2 and 3).